Pure & Appl. Chem., Vol.52, pp.713-727.
Pergamon Press Ltd. 1980. Printed in Great Britain.

0033-4545/80/0301-0713$02.00/0

STEREOELECTRONIC MODULATION OF DIOXYGEN COORDINATION

T. Yoshida, K. Tatsumi, and Sei Otuska

Department of Chemistry, Faculty of Engineering Science, Osaka University, Toyonaka, Osaka, Japan 560.

Abstract - A survey of molecular geometries of a series of planar nickel triad complexes $L_2M(AA)$ (L=monodentate donor ligands, e.g., RNC, PR_3; AA= two center acceptor ligands, e.g., PhC≡CPh, PhN=NPh, O_2 etc.) has led to the finding of a general trend which may be called the inter-ligand angle effect. The inter-ligand angle LML becomes wider as the electron-accepting ability of AA decreases. Conversely, an electronegative AA calls for a narrower LML angle. Thus the dioxygen complex L_2MO_2 shows the smallest LML angle (∿90°). When the steric bulk of L forces a wider LML angle, then η^2-O_2 coordination bond may be weakened. O_2 coordination is reversible for $PdO_2[PPh(t\text{-}Bu)_2]_2$ (PPdP=115.4°), while it is irreversible for $PtO_2[PPh(t\text{-}Bu)_2]_2$ (PPtP=113.1°). Semi-empirical MO calculations at a level of a modified INDO approximation were carried out on model compounds, $L_2M(AA)$ (L=HNC, PH_3), to give insight into the nature of O_2-metal bonding and to provide a rationale for the inter-ligand angle effect. The calculations show a minimum in total energy of L_2MO_2 (M=Ni, Pd; L=PH_3) at an LML angle of 107°. The metal-acceptor ligand bond indices were also calculated for varying LML angle. The effect on the LML angle was discussed in terms of a second order perturbational treatment.

INTRODUCTION

Neutral d^{10} nickel triad compounds of type ML_n having electron donating ligands L doubtless belong to a class of compounds characterized by strong nucleophilicity. They form a variety of complexes of formula $M(\eta^2\text{-}AA)L_n$ with two-center π-acids AA such as olefins, acetylenes, diazenes, dioxygen etc. (Ref. 1,2). As reported by Tolman (Ref. 3) for a series of olefin complexes $M(\eta^2\text{-olefin})L_2$, there is in general a simple linear relationship between the formation constants (log K) and the energy level of the lowest unoccupied orbital of free olefins. The energy of the π_g^* orbitals of dioxygen is certainly lower than that of the π* levels of most olefins. Therefore it was surprising to find a reversible coordination of dioxygen in a palladium compound $Pd[PPh(t\text{-}Bu)_2]_2$ (Ref. 4,5). Steric congestion in the dioxygen compound $PdO_2[PPh(t\text{-}Bu)_2]_2$ may be invoked to account for the facile dioxygen release. However, a platinum analogue $PtO_2[PPh(t\text{-}Bu)_2]_2$ was found to bind dioxygen irreversibly (Ref. 4.5). Thus, intramolecular steric congestion cannot be the sole factor governing the M-O_2 bond strength. Previously we reported molecular orbital studies on $Ni(\eta^2\text{-}AA)(HNC)_2$ (AA=HC≡CH, HN=NH, O_2) at the modified INDO calculation level (Ref. 6,7). In order to provide a rationale for the above observations, we investigated the effect of complex geometries, in particular the inter-ligand angle LML, on the coordination of dioxygen, in terms of the modified INDO method (Ref. 5).

MOLECULAR STRUCTURE

Several dioxygen complexes MO_2L_2 have been studied by X-ray analysis (Ref. 5,8,9). Their important structural parameters are summarized in Table 1. The O-O distances ranges from 1.45 to 1.37 Å. The O-O distance of $PdO_2[PPh(t\text{-}Bu)_2]_2$ is slightly shorter than that of $PtO_2[PPh(t\text{-}Bu)_2]_2$. The O-O bond lengths in Ir(I) and Rh(I) complexes fall within a range of 1.41 to 1.52 Å (Ref. 10,11). In the free dioxygen molecule there is a correlation, called Badger's rule (Ref. 12), between the force constant $f_{O\text{-}O}$ and the O-O distance. The force constants of $PtO_2(PPh_3)_2$ and $NiO_2(t\text{-}BuNC)_2$ are 3.0 and 3.5 mdyne/Å, respectively (Ref. 13). The O-O distances in both complexes (Table 1) being comparable (∿1.45 Å), it is apparent that the distance is rather insensitive to the electronic perturbation caused by coordination to a "soft" late-transition metal.

The dihedral angle between the normal to the MO_2 plane and the normal to the MP_2 plane is 6.8° for $PdO_2[PPh(t\text{-}Bu)_2]_2$ and 2.7° for the platinum congener. The inter-ligand angle LML is 115.4(2)° for the former and 113.1(2)° for the latter. The difference, albeit small, is beyond esd and significant. Note the smaller angle (101.2°) for $Pt(O_2)(PPh_3)_2$ and the much smaller angle (91.8°) for $Ni(O_2)(t\text{-}BuNC)_2$.

MOLECULAR ORBITALS

Here we first review briefly the MO level diagrams of nickel complexes $Ni(AA)L_2$ (L=HNC) (Ref. 8,9), where AA is a representative π-acid, i.e. acetylene, hypothetical diimine (HN=NH), and dioxygen, and discuss the M-AA bonding. The comparative MO analysis should contribute to our better understanding of the $M\text{-}O_2$ bond nature. Structural parameters of these hypothetical compounds (Figure 1) were taken respectively from the X-ray data of $Ni(PhC{\equiv}CPh)(t\text{-}BuNC)_2$ (Ref. 14), $Ni(PhN{=}NPh)(t\text{-}BuNC)_2$ (Ref. 15), and $NiO_2(t\text{-}BuNC)_2$ (Ref. 9). Note the <u>trans</u> configuration of the coordinated diimine. We shall then show the MO of phosphine compounds $MO_2(PH_3)_2$ (M=Ni, Pd) and the dependence of the total energy on the inter-ligand angle PMP.

Method of Calculation

The ASMO SCF method at the level of INDO approximation (Ref. 6,16) was applied quite satisfactorily to some first and second row transition metal compounds. The order of orbital energy levels and the pattern of populations provided was essentially identical with those

Table 1. Geometry of MO_2L_2

Complex	O-O(Å)	M-O(Å)	M-L(Å)	LML(°)	Ref.
$\{Pd(O_2)[PPh(t\text{-}Bu)_2]_2\}\cdot C_7H_8$	1.37(2)	2.05(2) 2.06(2)	2.357(5) 2.360(5)	115.4(2)	5
$\{Pt(O_2)[PPh(t\text{-}Bu)_2]_2\}\cdot C_7H_8$	1.43(2)	2.02(2) 2.02(2)	2.290(4) 2.290(4)	113.1(2)	5
$[Pt(O_2)(PPh_3)_2]\cdot 2CHCl_3$	1.45(4)	2.01(2) 2.01(2)	2.233	101.2(4)	8
$Ni(O_2)(t\text{-}BuNC)_2$	1.45(1)	1.81(1)		91.8(5)	9

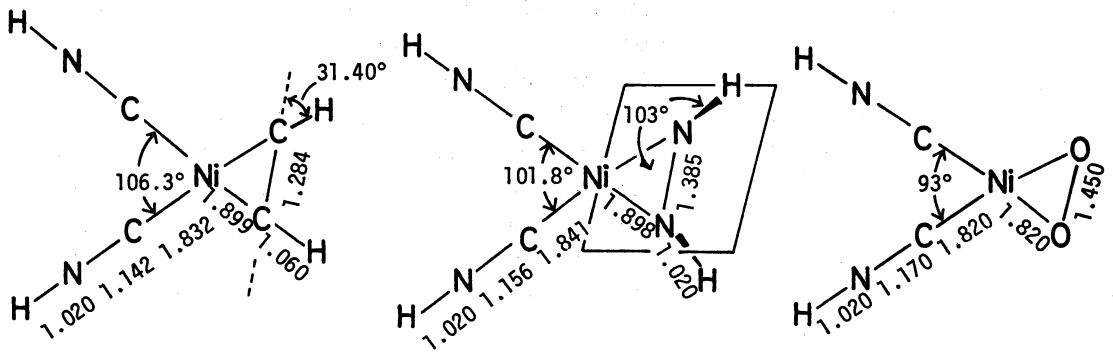

Fig. 1 Structure of $Ni(AA)(HCN)_2$ (AA=HC≡CH, HN=NH, O_2)

given by ab initio calculations. Details of the calculation have been given elsewhere (Ref. 6,7,16). When orbital relaxation upon ionization does not affect the orbital level sequence significantly, our calculations (Ref. 16) provide energy schemes of such complexes as $Ni(CO)_4$, $Cr(CO)_6$, and $Mo(CO)_6$ which accord with the photoelectron spectra even better than do the ab initio and MSW=X_α calculations.

Comparison of Ni-π-Acid Bonding

In Figure 2 the frontier orbitals (Ref. 6,7) of $Ni(\eta^2\text{-AA})(HNC)_2$ are shown. The LUMO, $\Psi_{21}(b_2)$ of the acetylene complex and $\Psi_{22}(b)$ of the diimine complex, consists primarily of the isocyanide $\pi^*(\perp)$ orbital with appreciable Ni $4p_y$ character, whereas the LUMO $\Psi_{22}(b_2)$ of the dioxygen compound consists of Ni $4p_y$ and isocyanide $\pi^*(\perp)$ with appreciable O_2 $\pi_u(\perp)$ character.

The HOMO $\Psi_{20}(b_1)$ for the acetylene and $\Psi_{21}(b)$ for the diimine complex is comprised of the Ni $3d_{xz}$ and the π-acid ligand $\pi_g^*(//)$ orbitals. These are typical of back-donation type bonding. For the dioxygen compound the HOMO $\Psi_{21}(a_2)$ is derived almost exclusively from the O_2 lone pair orbital $\pi_g^*(\perp)$ and the back-donation type orbital $\Psi_{20}(b_1)$ lies slightly below this HOMO.

In Table 2 we show the charge distribution of valence electrons over the nickel s,p, and d orbitals as well as the ligand atoms. These results give the apparent configuration of nickel as follows (L=HNC) (Ref. 6).

$$Ni(HC{\equiv}CH)L_2 : (3d)^{8.90}(4s)^{0.52}(4p)^{1.07}$$
$$Ni(HN{=}NH)L_2 : (3d)^{8.80}(4s)^{0.53}(4p)^{0.99}$$
$$Ni(O_2)L_2 : (3d)^{8.49}(4s)^{0.54}(4p)^{0.98}$$

Note that the major difference lies in the d-orbital occupation, which is governed almost exclusively by the population of the inplane d_{xz} orbital. Consistently the charge density on the atomic orbitals of the unsaturated bonds increases in the order, HC≡CH < HN=NH < O_2.

Table 3 summarizes π-orbital populations (q) on the complexed and free π-acid ligands. As previously defined (Ref. 6), Δ_q is the difference in population between the bonding π and

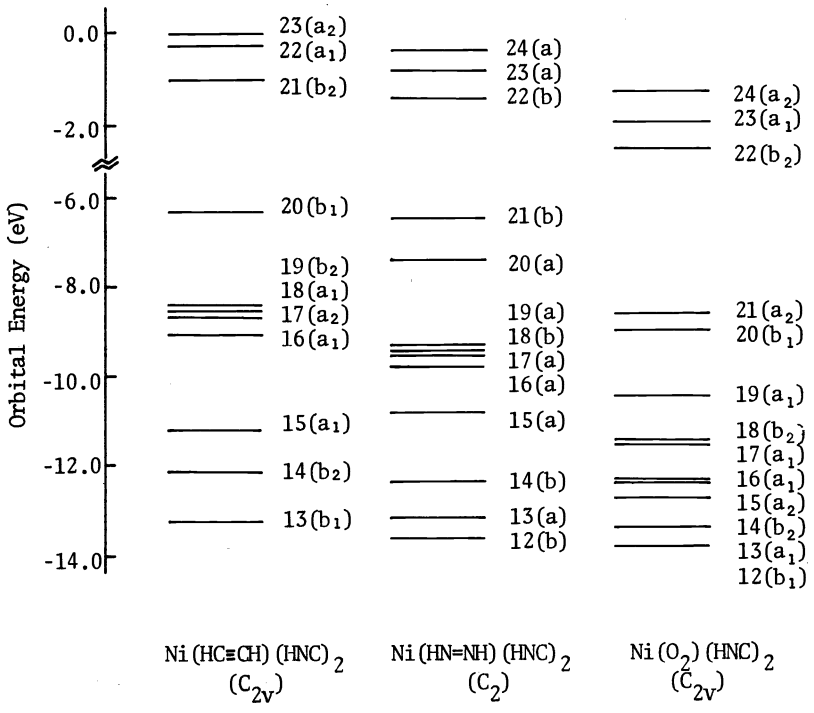

Fig. 2 Upper portions of the molecular orbital level diagrams for $Ni(HC{\equiv}CH)(HNC)_2$, $Ni(HN{=}NH)(HNC)_2$, and $Ni(O_2)(HNC)_2$. The highest occupied levels are $20(b_1)$, $21(b)$, and $21(a_2)$, respectively.

Table 2. Calculated Electron Distributions for $Ni(C_2H_2)L_2$, $Ni(N_2H_2)L_2$, and $Ni(O_2)L_2$ (L=HNC)

Atom	Atomic Orbital	Charge Density		
		$Ni(C_2H_2)L_2$	$Ni(N_2H_2)L_2$	$Ni(O_2)L_2$
Ni	s	0.517	0.529	0.537
	p	1.065	0.991	0.975
	d_{xz}	1.151	0.966	0.580
	d_{yz}	1.928	1.957	1.978
	d_{xy}	1.960	1.974	1.988
	$d_{x^2-y^2}$	1.951	1.965	1.982
	d_{z^2}	1.912	1.933	1.959
C(C≡C)	s, p	4.155		
H	s	0.916		
N(N=N)	s, p		5.348	
H	s		0.851	
O(O=O)	s, p			6.473
C(CNH)	s, p	3.021	3.897	3.860
N	s, p	4.964	4.953	4.923
H	s	0.801	0.794	0.780

Table 3. Orbital Populations (q) on Ligand π-orbitals in $Ni(AA)L_2$ (L=HNC)

q[a]	$Ni(C_2H_2)L_2$	C_2H_2	$Ni(N_2H_2)L_2$	N_2H_2	NiO_2L_2	$O_2(^3\Sigma_g^-)$	O_2^-
$\pi_u(\perp)$	1.86	2.00			1.88	2.00	2.00
$\pi_u(//)$	1.70	2.00	1.81	2.00	1.89	2.00	2.00
$\pi_g^*(\perp)$	0.00	0.00			2.00	1.00	(3.00)
$\pi_g^*(//)$	0.63	0.00	0.94	0.00	1.46	1.00	
Δ_q[b]	2.92	4.00	0.87	2.00	0.30	2.00	1.00
D(A-A)[c]	1.284	1.19	1.385	1.243	1.45	1.20	1.28

a. $q(\pi_u(\perp)) = 4\sum_{i(a_2)}^{occ} c^2_{io(p_y)}$, $q(\pi_u(//)) = 4\sum_{i(a_1)}^{occ} c^2_{io(p_z)}$, $q(\pi_g^*(\perp)) = 4\sum_{i(b_2)}^{occ} c^2_{io(p_y)}$, $q(\pi_g^*(//)) = 4\sum_{i(b_1)}^{occ} c^2_{io(p_z)}$. b. See text. c. Observed A-A distances (Å).

anti-bonding π* orbitals (eq 1).

$$\Delta_q = q(\pi_u(\perp)) + q(\pi_u(//)) - q(\pi_g^*(\perp)) - q(\pi_g^*(//)) \quad (1)$$

$$\Delta(\Delta_q) = \Delta_q(\text{complexed}) - \Delta_q(\text{free}) \quad (2)$$

The $\Delta(\Delta_q)$ value (eq 2) should then reflect the A-A bond length variation. Indeed there is an approximately linear relation between the bond length ratio γ defined by equation 3 and the $\Delta(\Delta_q)$ value for a series $Ni(\eta^2\text{-}AA)L_2$ (L=t-BuNC, PPh_3; AA=O_2, PhN=NPh, PhC≡CPh, CH_2=CH_2) (Ref. 6).

$$\gamma = \frac{R_{A=A}(\text{complex}) - R_{A=A}(\text{free})}{R_{A-A}(\text{saturated}) - R_{A=A}(\text{free})} \quad (3)$$

Electronic Effect of the Ligand

The MO features so far described are not particularly impressive since they are consistent with the qualitative bond scheme proposed by Dewar, Chatt and Duncanson. However, when we examined the dependence of the bond indices W_{M-A} on the electron donating ability of the ligand L in $Ni(AA)L_2$, an interesting phenomenon emerged. By changing the valence-state ionization potential (I_S^H) of the hydrogen atom of the hypothetical ligand, hydrogen isocyanide, we mimiced the variation of electronic donating or accepting ability of the isocyanide ligand. For I_S^H lower than 13.6 eV, the isocyanide should be more electron donating than HNC. The electronic effects on the bond indices W_{Ni-A} are seen in Figure 3 (Ref. 6). Note the unique behavior of W_{Ni-O}; the greater the electron donation of HNC, the less is the Ni-O bond strength. This is contrary to what we expect from the conventional Dewar-Chatt-Duncanson bonding scheme. These features (Figure 3) are a natural consequence of the relative level position of the O_2 acceptor orbital and the donor orbital (b_1) of the fragment species $Ni(HNC)_2$, as shown in Figure 4. A UHF-INDO calculation was performed for the elongated O_2 (1.45 Å) and the bent $Ni(HNC)_2$ species separately in order to confirm the relative energy levels. The latter was assumed to be in the lowest triplet state with its geometry as in Figure 1. The resulting HOMO (degenerate) of the α-spin orbital for O_2 was found to be at

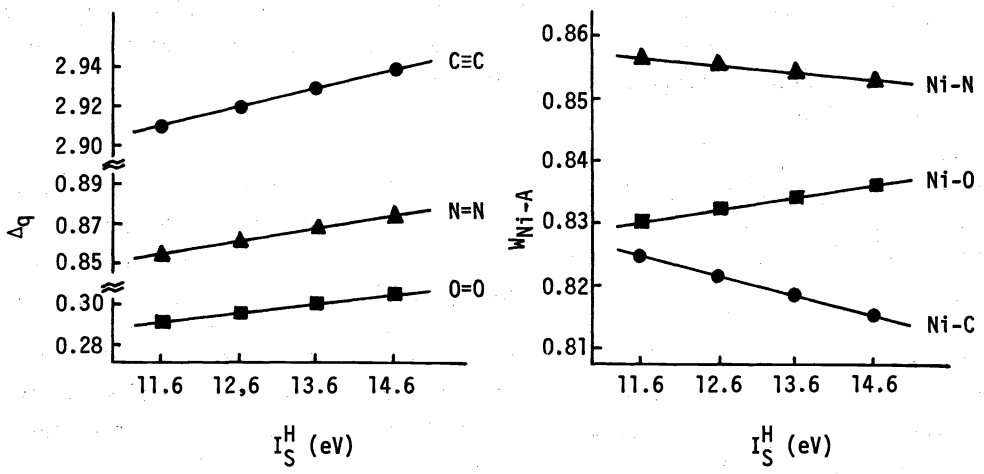

Fig. 3 Variations of the Δ_q values (left) and bond indices W (right) as the functions of I_S^H. ●: Ni(HC≡CH)(HNC)$_2$, ▲: Ni(HN=NH)(HNC)$_2$, ■: Ni(O_2)(HNC)$_2$.

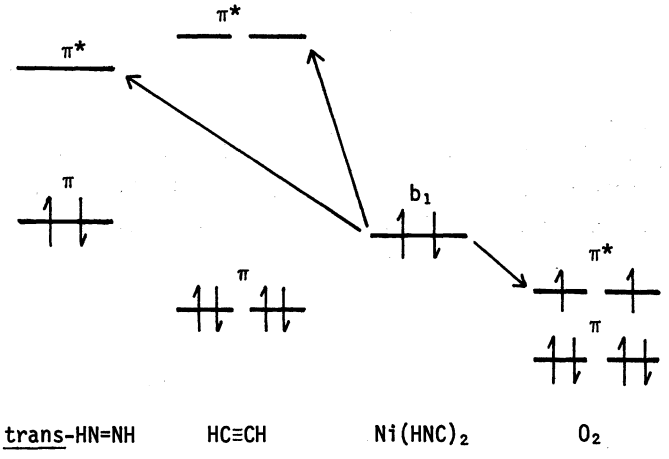

Fig. 4 Schematical level diagrams for the π and π* orbitals of trans-HN=NH, HC≡CH, and O_2 as well as the highest b_1 orbitals of Ni(HNC)$_2$. The back-donation of electrons occurs in the direction of the arrows.

-12.05 eV, while that for Ni(HNC)$_2$ at -6.21 eV (Ref. 6).

The trend that the M-O_2 bond strength decreases with increase in electron donating ability of the metal fragment is also observable for various dioxygen rhodium compounds (Ref. 17). ν(Rh-O) increases as the electron accepting ability of the ligands is enhanced. This contrasts to Vaska's dioxygen compounds where the reversibility of dioxygen coordination was realized for iridium complexes having electron-accepting ligands (Ref. 18). The reversibility, however, may not necessarily reflect the thermodynamic stability or the metal-dioxygen bond strength.

In IrCl(O_2)(CO)(PPh_3)$_2$, the dioxygen ligand lies in the equatorial plane with Cl and CO, the

electron donating phosphines being in the axial positions. No theoretical account has been given for this site preference of dioxygen in the Vaska's complex. It can be accounted for in terms of such an electronic effect as seen in Figure 3.

Geometrical Effect in the Ligand

MO level diagrams for $MO_2(PH_3)_2$ (M=Ni, Pd) were similarly calculated (Ref. 5). The frontier orbitals are shown in Figure 5. In the case of $PdO_2(PH_3)_2$, the HOMO, $\Psi_{19}(b_1)$, comprised from the Pd d_{xz} and O_2 $\pi_g^*(//)$ orbital, is almost degenerate with $\Psi_{18}(a_2)$, which has strong O_2 $\pi_g^*(\perp)$ character. The level scheme for $NiO_2(PH_3)_2$ is very similar to that for $NiO_2(HNC)_2$.

The total energy of $M(AA)L_2$ depends on the inter-ligand angel θ. This is illustrated for $MO_2(PH_3)_2$ (Figure 6). The angular dependence of bond indices and π-orbital populations was also calculated. The bond index W_{M-O} decreases monotonically as the angle θ increases ($90° > \theta > 150°$), while both W_{M-P} and W_{O-O} increase with increase in θ (Ref. 5).

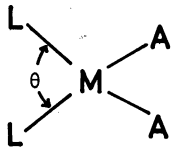

REVERSIBLE COMPLEXES

$PdO_2[PPh(t\text{-}Bu)_2]_2$

Two coordinate compounds $M[PPh(t\text{-}Bu)_2]_2$ (M=Pd, Pt) dissolved in toluene or hexane absorb dioxygen rapidly at low temperature to form the corresponding dioxygen complexes $MO_2[PPh(t\text{-}Bu)_2]_2$, which can be recrystallized from toluene. A pale green solution of $PdO_2[PPh$-

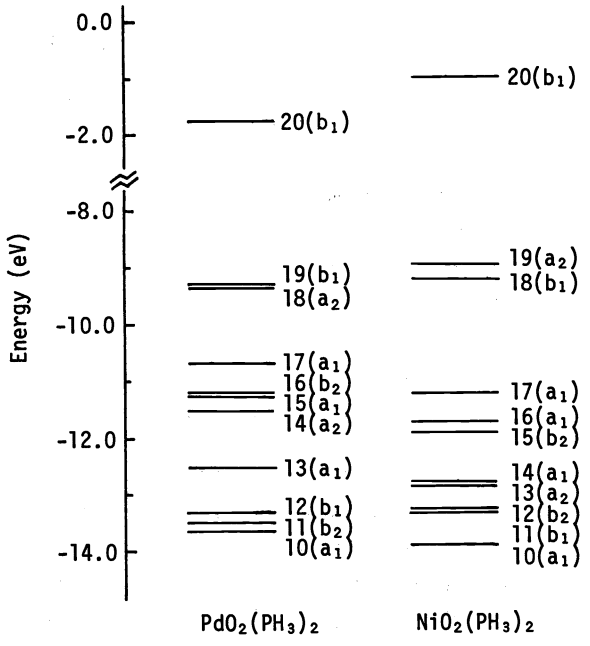

Fig. 5 Upper portions of molecular orbital level diagrams for $MO_2(PH_3)_2$ (M=Pd, Ni).

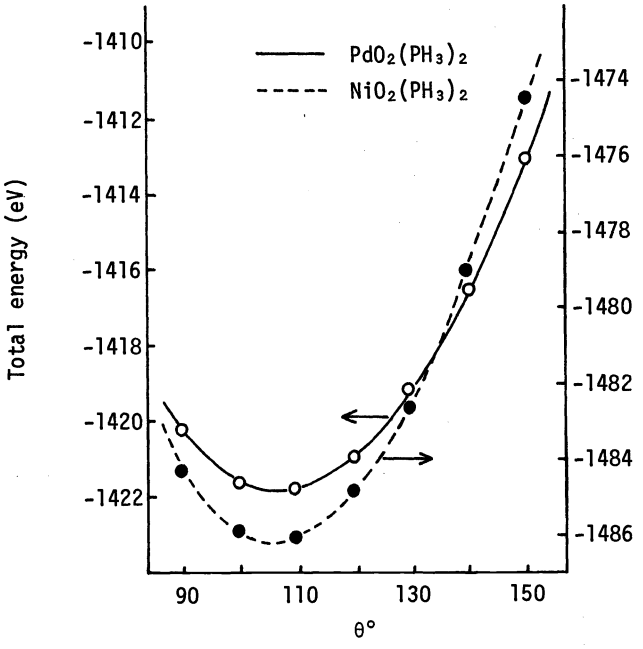

Fig. 6 Total energy calculated for $MO_2(PH_3)_2$ with varying the inter-ligand angle(θ).

$(t\text{-}Bu)_2]_2$ in methanol was heated at 60° for 2 h. From the brownish solution was isolated the parent compound $Pd[PPh(t\text{-}Bu)_2]_2$ in 64 % yield. The dioxygen dissociation was also observed upon heating the crystalline $PdO_2[PPh(t\text{-}Bu)_2]_2$ at 60°-70° under high vacuum (10^{-3} mmHg) for 38 h, as detected by the complete disappearance of ν(O-O)(915 cm^{-1}).

The dioxygen coordination in platinum analogue $PtO_2[PPh(t\text{-}Bu)_2]_2$ similarly prepared from $Pt[PPh(t\text{-}Bu)_2]_2$ was found to be irreversible.

$[PdO_2(L\text{-}L)]_2$

The ligands L-L are newly prepared 1,4-bis(di-tert-butylphosphinopropyl)benzene(BPPB) and 1,4-bis(di-tert-butylphosphinobutyl)benzene(BPBB). Attempts to obtain mononuclear Pd(0) compounds, Pd(L-L), have failed. The following substitution reaction was attempted in high dilution. The product isolated was a dimer $[Pd(L\text{-}L)_2]_2$, as determined by cryoscopic molecular weight measurements. Their ^1H nmr spectra are consistent with the trans-alignment of the phosphorus atoms. A single crystal X-ray analysis confirmed the dimeric structure (Ref. 19).

$$Pd(\eta\text{-}C_3H_5)(\eta\text{-}C_5H_5) + L\text{-}L \longrightarrow Pd(L\text{-}L) \qquad (4)$$

Most likely the molecular structure is retained in solution.

They form dioxygen compounds $[PdO_2(L\text{-}L)]_2$ which can be characterized by ir(ν(O-O) 900 cm^{-1} for n=3,4), ^1H nmr, elemental analysis and molecular weight measurements. Some spectral data are summarized in Table 4.

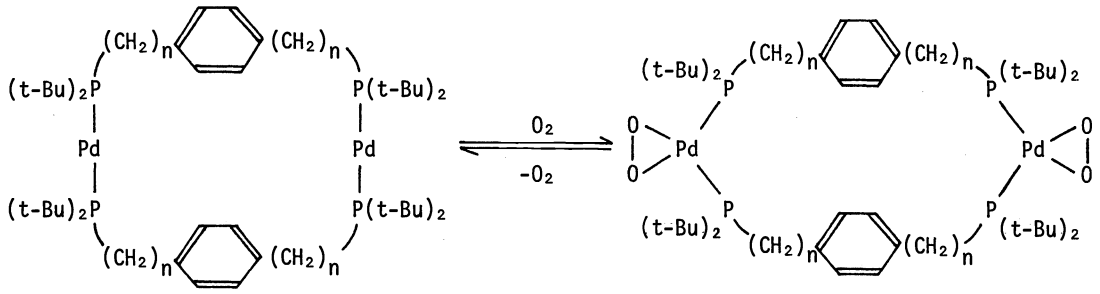

n=3 : $[Pd(BPPB)]_2$
n=4 : $[Pd(BPBB)]_2$

n=3 : $[PdO_2(BPPB)]_2$
n=4 : $[PdO_2(BPBB)]_2$

Dioxygen release from $[PdO_2(BPPB)]_2$ was observed upon heating the methanol solution at 50°, as monitored by the disappearance of the ν(O-O) band, the parent compound $[Pd(BPPB)]_2$ being recovered (about 50 %). Heating solid $[PdO_2(BPBB)]_2$ under high vacuum (10^{-3} mmHg) for 20 h, the ν(O-O) also disappeared. The parent compound was not recoverable, however, due to extensive decomposition to ill-defined substances.

INTER-LIGAND ANGLE EFFECTS

The various factors affecting the inter-ligand angle LML in existing planar complexes $M(\eta^2\text{-}AA)L_2$ will be briefly discussed here.

The ir N≡C stretching frequencies of isocyanide complexes $Ni(\eta^2\text{-}AA)(RNC)_2$ provide a sensitive probe of the π-acidity of π-ligand AA (Ref. 1). Values of ν(N≡C) of about 2000 cm^{-1} correspond to formally Ni(0) systems, while values near 2200 cm^{-1} correspond to Ni(II). The higher ν(N≡C) values are thus associated with stronger π-acidity of AA. An approximately linear correlation exists between the ν(N≡C) values and the electronegativities of such π-ligands as

Table 4. Spectral Data of $[PdO_2(L\text{-}L)]_2$ (L-L=BPPB[a], BPBB[a])

Complex	Color	^{1}H NMR, δ (ppm, Me_4Si)[b]				IR, cm^{-1}[c]
		t-Bu	J_{P-H}(Hz)	-CH_2-	Ar	ν(O-O)
$[PdO_2(BPPB)]_2$	Yellowish-green	1.37(d)	12.7	2.1(br), 1.8(br), 1.6 ∿ 1.0(br)	6.96(s)	900(s), 875(m)
$[PdO_2(BPBB)]_2$	Yellowish-green	1.37(d)	12.7	2.5(br), 1.8(br), 1.6 ∿ 1.0(br)	6.98(s)	900(s), 875(m)

a. See text. b. Measured in CD_2Cl_2. c. Measured in Nujol mull.

olefins and diazo compounds. Hence the relationship may be useful for assessing electronegativities of unknown π-acids. The position of the dioxygen ligand, however, deviates from this line. This is not unexpected since the nature of $M-O_2$ bonding differs from that of M-olefin bonding, as manifested in the frontier orbital compositions as well as in the bond indices W_{M-A} (vide supra). The known ν(N≡C) and CNiC angles (θ) are shown in Table 5. Apart from the position of dioxygen the plots of ν(N≡C) vs θ give a parabolic curve (Figure 7). The θ values of MO_2L_2 are narrower than expected from this curve due to an efficient electron transfer (nearly 1.5 electrons) required by dioxygen. Although there exists no simple correlation for a broad category of π-ligands, the following qualitative generalization can be made: The stronger the electron-accepting property of the π-ligand AA, the smaller is the inter-ligand angle θ.

Table 5. Isocyanide Stretching Frequencies and Inter-Isocyanide Ligand Angles (θ) in Complexes, $Ni(t\text{-}BuNC)_2(AA)$

AA	Ni-C, Å	ν(N≡C), cm^{-1}	θ, deg
PhC ≡ CPh	1.83 (3)	2138, 2110	106.3 (16)
PhN = NPh	1.841 (5)	2168, 2140	101.8 (2)
$C_{13}H_8N_2$ [a]	1.844 (4)	2180, 2158	100.4 (2)
$(CN)_2C = C(CN)_2$	1.866 (5)	2194, 2179	98.9 (2)
O_2	1.84 (1)	2196, 2178	91.8 (5)

[a] diazofluorene

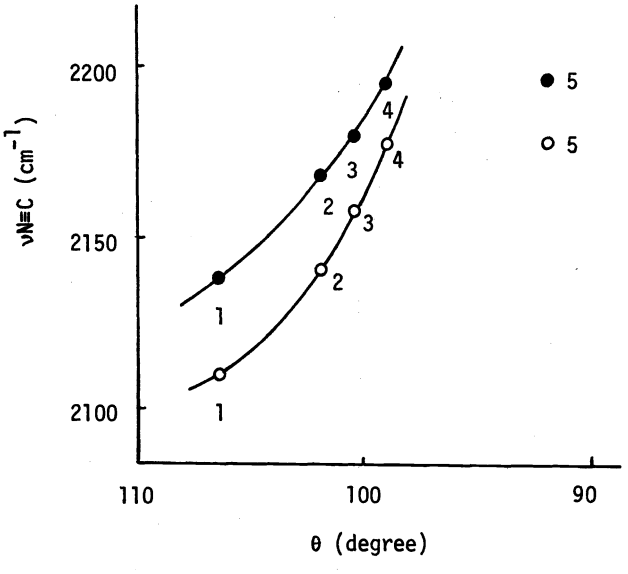

Fig. 7 Plots of νC≡N (●, a-mode; ○, b-mode) vs. inter-ligand angle of $Ni(AA)(t\text{-}BuNC)_2$. 1, PhC≡CPh; 2, PhN=NPh; 3, diazofluorene; 4, TCNE; 5, O_2.

A similar trend is observed for phosphine complexes of type $Pt(\eta^2\text{-AA})(PPh_3)_2$, as shown in Table 6. The electronic capacity of the metal also affects the PMP angle in $M(\eta^2\text{-AA})(PPh_3)_2$, as can be seen in Table 7. Note the angle trend, Ni < Pt; Pt < Pd.

An account of the facile dissociation of dioxygen from $PdO_2[PPh(t\text{-}Bu)_2]_2$ and $[PdO_2(L\text{-}L)]_2$ (L-L=BPPB, BPBB) can now be given in terms of the electronic and geometrical effects. (1) The electron donating ability of $PPh(t\text{-}Bu)_2$, compared to PPh_3, does not contribute to increasing the M-O_2 bond strength, compared to that of the irreversibly binding $PdO_2(PPh_3)_2$. (2) The wide PMP angle reduces the M-O_2 bond strength, as has already been described in terms of the bond indices $W_{M\text{-}O}$ (the preceding section). In fact, the PPdP angle is, albeit small, greater than the PPtP angle. This effect, of geometrical origin, may be regarded as a stereoelectronic effect. The LML angle can be changed to some extent by appropriate design of steric bulk of monodentate ligands or by a choice of geometries of bidentate ligands, so as to modify the M-A_2 bond strength. This type of approach may be called stereoelectronic modulation of coordination.

Table 6. Inter-Ligand Angles and Metal-Ligand Bond Lengths in $Pt(\eta^2\text{-AA})(PPh_3)_2$

AA	PPtP(θ°)	Pt-P(Å)	Ref.
O=O	101.2	2.233	8
$(NC)_2C=C(CN)_2$	101.4	2.290	20
NCCH=CHCN	104.4	2.287	21
$CF_3CF=CFCF_3$	104.7	2.312	22
$CH_2=C=CH_2$	107.1	2.282	23
S=C=S	107.1	2.29	24
$P\text{-}NO_2C_6H_4CH=CHC_6H_4(p\text{-}NO_2)$	109.5	2.28	25
$CH_2=CH_2$	111.6	2.268	26

Table 7. Inter-Ligand Angles and Metal-Ligand Lengths in $M(\eta^2\text{-AA})(PPh_3)_2$

M	AA	PMP(θ°)	M-P(Å)	Ref.
Ni	$CH_2=CH_2$	110.5	2.152	27
Pt	$CH_2=CH_2$	111.6	2.268	26
Pd	$CH_2=C=CH_2$	109.3	2.314 2.324	28
Pt	$CH_2=C=CH_2$	107.1	2.278 2.286	23
Pd	S=C=S	108.8	2.316 2.415	29
Pt	S=C=S	107.1	2.346 2.240	24

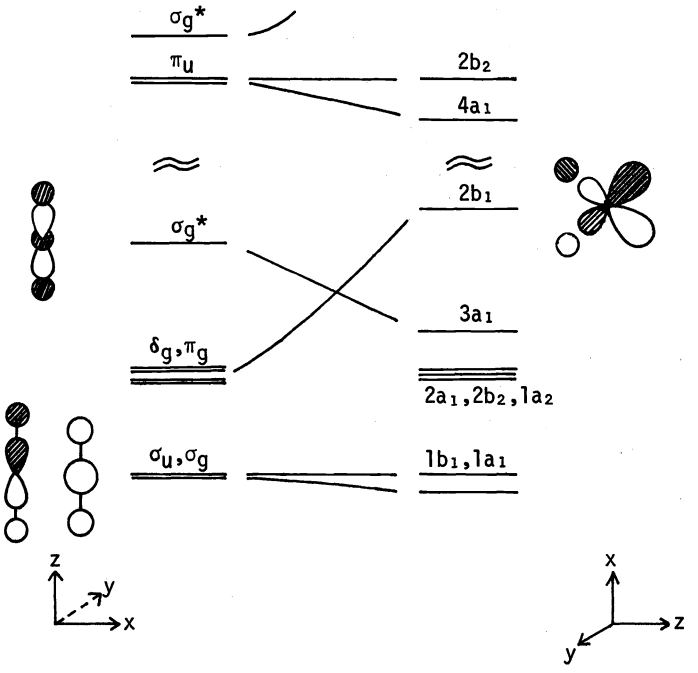

Fig. 8 Walsh diagram of ML_2

The origin of this effect can be delineated as follows. A qualitative Walsh diagram of the valence orbitals of ML_2 ($M=d^{10}$ metals) (Ref. 30) is given in Figure 8. The most conspicuous change is the destabilization of the inplane b_1 orbital, comprized mainly of d_{xz} and p_x, with decreasing LML angle. The mixing of p_x with d_{xz} (hybridization) is achieved in second order through mixing with ligand orbitals. Theoretical analyses of this type of orbital mixing have already been given by Hoffmann (Ref 31), Mingo (Ref. 32), and Fukui (Ref. 33). If a π-ligand demands strong back donation from the metal center, this can be achieved by narrowing the LML angle, viz. raising the b_1 level. Another important frontier orbital of ML_2 which must be considered for the interaction with π-ligand AA is the a_1 type orbital comprized mainly of the metal d_{z^2} and s orbitals. These orbitals change their directionality (and hybridization) when the linear ML_2 is bent, as shown schematically below (see also Figure 8).

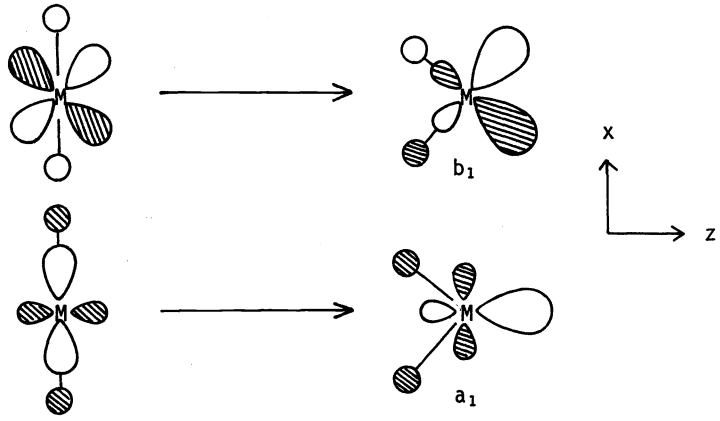

For simplicity we assume that the stabilization to be gained upon interaction of ML_2 with AA derives mainly from two interactions, i.e., donation (a_1) and back donation (b_1). The stabilization energies can then be given by a second order perturbation treatment (eq. 5).

$$\Delta E = \Delta E_{a_1} + \Delta E_{b_1} = -\frac{2\langle a_1|H'|\pi\rangle^2}{|\varepsilon_{a_1} - \varepsilon_{\pi}b|} - \frac{2\langle b_1|H'|\pi^*\rangle^2}{|\varepsilon_{b_1} - \varepsilon_{\pi^*}|} \qquad (5)$$

As θ decreases, the overlap dependent numerators $\langle a_1|H'|\pi\rangle$ and $\langle b_1|H'|\pi^*\rangle$ both increase in magnitude. Obviously $|\varepsilon_{a_1}|<|\varepsilon_{\pi}|$ for all π-ligands (note negative values for ε). As θ decreases, the a_1 orbital of ML_2 is stabilized, resulting in a decrease in $|\varepsilon_{a_1} - \varepsilon_{\pi}|$. Hence the donor interaction (a_1) increases with bending of ML_2.

The situation for the second term ΔE_{b_1} is more complex. There are two cases. (1) $|\varepsilon_{b_1}| > |\varepsilon_{\pi^*}|$ as is the case for most olefins, acetylenes, diazenes etc. and (2) $|\varepsilon_{b_1}|<|\varepsilon_{\pi^*}|$ as is the case for dioxygen. In the former case, destabilization of the b_1 orbital of ML_2 will decrease $|\varepsilon_{b_1} - \varepsilon_{\pi^*}|$, resulting in increase of ΔE_{b_1}. In the latter case, on the contrary, the b_1 destabilization increases the $|\varepsilon_{b_1} - \varepsilon_{\pi^*}|$ value. However, it is not immediately obvious whether the contribution of the denominator to ΔE_{b_1} exceeds to that of the numerator. Therefore we calculated two bond indices $W_{Ni\text{-}A(a_1)}$ and $W_{Ni\text{-}A(b_1)}$ separately for $Ni(\eta^2\text{-}AA)(HNC)_2$ ($AA=C_2H_2$, N_2H_2, O_2). The results are shown in Figure 9. The values of $W_{Ni\text{-}A(a_1)}$ increase with decrease in θ, as expected. The values of $W_{Ni\text{-}A(b_1)}$ also increase with decrease in θ, with the least slope for the dioxygen complex $NiO_2(HNC)_2$. Therefore one can conclude that even for the case $|\varepsilon_{b_1}|<|\varepsilon_{\pi^*}|$, the π-type interaction contributes to the M-A bonding due to its effective overlap.

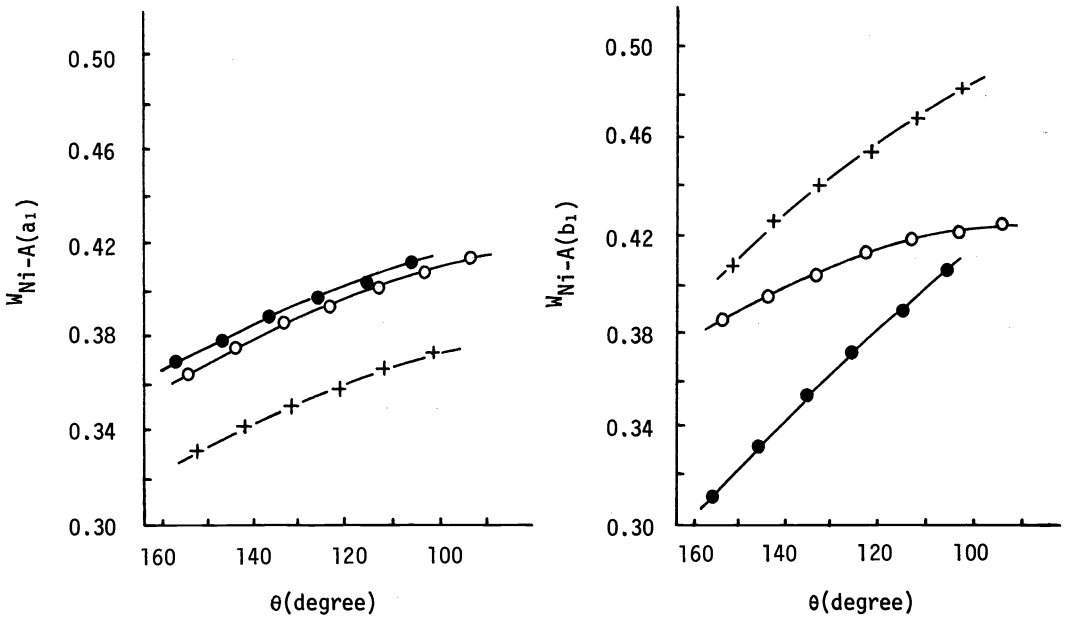

Fig. 9 Variation of $W_{Ni\text{-}A(a_1)}$ and $W_{Ni\text{-}A(b_1)}$ in $Ni(AA)(HNC)_2$ as a function of inter-ligand angle (θ). AA =HC≡CH(●), O_2(○), HN=NH(+).

Let us examine the effect of electron donation or acceptance by auxiliary ligands L. The enhanced electron donating capability of L raises the b_1 level of ML_2 relative to that of ML_2 with a poorly donating L. Therefore the same degree of back donation can be achieved with a relatively wider LML angle. Theoretically, it is predicted for one type of π-ligand that in $M(\eta^2\text{-AA})L_2$, the LML angle should increase with increasing electron donating ability of L. Unfortunately, there are no appropriate structural data to confirm this prediction. A caution must be made. The argument here assumes a constant M-L distance. A change in electronic character of L is often accompanied by a change in M-L distance. For example, the Ni-P distances of $Ni(C_2H_4)(PPh_3)_2$ (Ref. 27) and $Ni(C_2H_4)[P(O\text{-}o\text{-}MeC_6H_4)_3]_2$ (Ref. 34) are 2.152(5) and 2.095(2) Å, respectively. With its short M-P distance, the phosphite ligand renders ML_2 (L=phosphite) species a good π-donor. This is manifested in the longer C=C distance (1.46(2) Å) of the ethylene ligand, compared to that (1.43(1) Å) of $Ni(C_2H_4)(PPh_3)_2$ (σπ synergic interactions may also be invoked). The steric bulk of PPh_3 and $P(O\text{-}o\text{-}MeC_6H_4)_3$ being comparable (Ref. 34,35), it may be of interest to compare the PNiP angle. The angle is 110.5° for $Ni(C_2H_4)(PPh_3)_2$, whereas 116.5° for $Ni(C_2H_4)[P(O\text{-}o\text{-}MeC_6H_4)_3]_2$. This feature does not invalidate our prediction, in view of the significant difference in M-P bond length. It appears that the short M-P distance offsets the effect of a wide PNP angle.

CONCLUSION

The inter-ligand angle LML of $M(\eta^2\text{-AA})L_2$ complexes is governed by the electronic properties and steric requirements of AA, L, and the identity of the metal. The angle variation enforced by the steric or geometrical requirements of L leads to modulation of various chemical properties of the complex. We have shown, inter alia, the effects on (1) the total energy and (2) the bond indices W_{M-A}. These modulations in turn reflect on the dissociative trend of π-ligand, e.g. dioxygen.

The MO level diagram will also be modulated by this geometrical factor, with many consequences; for example, electronic spectrum, redox property etc.

The geometrical effect is also observed for complexes of type MA_2L_2 (A=monodentate ligands, e.g. H^-). An example of interest is the change in hybridization of the metal center in PtH_2-(L-L) (L-L=chelating diphosphines), as manifested in the nmr coupling constant J(Pt-H) (Ref. 36).

The present analysis, suggests a rationale for the hitherto unexplained phenomenon of the chelate ring size effect operative in various homogeneous catalytic systems (Ref. 37). At least, recognition of this stereoelectronic effect should be of use in designing efficient homogeneous catalysts.

Acknowledgement - We thank Professor Ronald Hoffmann for critical reading this manuscript.

REFERENCES

1. For example, S. Otsuka, T. Yoshida, and Y. Tatsuno, J. Am. Chem. Soc., 93, 6462 (1971).
2. For a review see (a) S. D. Ittel and J. A. Ibers, Advan. Organometal. Chem., 14, 33 (1976); (b) P. W. Jolly and G. Wilke, "The Organic Chemistry of Nickel", Vol I, Chapter V, Academic Press, New York, (1974).
3. C. A. Tolman, J. Am. Chem. Soc., 96, 2780 (1974).

4. S. Otsuka and T. Yoshida, J. Am. Chem. Soc., 99, 3098 (1977).
5. T. Yoshida, K. Tatsumi, M. Matsumoto, K. Nakatsu, A. Nakamura, T. Fueno, and S. Otsuka, Nouveau J. Chim., in press.
6. K. Tatsumi, T. Fueno, A. Nakamura, and S. Otsuka, Bull. Chem. Soc. Jpn., 49, 2164 (1976).
7. K. Tatsumi, T. Fueno, A. Nakamura, and S. Otsuka, ibid., 49,2170 (1976).
8. T. Kashiwagi, N. Yasuoka, N. Kasai, M. Kakudo, S. Takahashi, and N Hagihara, Chem. Commun., 743 (1969).
9. M. Matsumoto and K. Nakatsu, Acta Crystallogr., B31, 2711 (1975).
10. M. J. Nolte, E. Singleton, and M. Laing, J. Am. Chem. Soc., 97, 6396 (1975).
11. M. Laing, M. J. Nolte, and E. Singleton, Chem. Commun., 660 (1975).
12. R. N. Badger, J. Chem. Phys., 2, 128 (1934); ibid., 3, 710 (1935).
13. A Nakamura, Y. Tatsuno, M. Yamamoto, and S. Otsuka, J. Am. Chem. Soc., 93, 6052 (1971).
14. R. S. Dickson, and J. A. Ibers, J. Organometal. Chem., 36, 191 (1972).
15. R. S. Dickson and J. A. Ibers, J. Am. Chem. Soc., 93, 4636 (1971); ibid., 94, 2988 (1972).
16. K. Tatsumi and T. Fueno, Bull. Chem. Soc. Jpn., 49, 929 (1976).
17. A. Nakamura, Y. Tatsuno, and S. Otsuka, Inorg. Chem., 11, 2058 (1972).
18. L. Vaska, Acc. Chem. Res., 9, 175 (1976).
19. T. Yoshida, H. Tamura, and S. Otsuka, to be publised.
20. G. Bombieri, E. Forsellini, C. Pannatoni, R. Graziani, and G. Bandoli, J. Chem. Soc. (A), 1313 (1970).
21. C. Pannatoni, R. Graziani, C. Bandoli, D. A. Clemente, and U. Belluco, J. Chem. Soc. (B), 371 (1970).
22. J. M. Balaban and J. A. McGinnety, J. Am. Chem. Soc., 97, 4232 (1975).
23. M. Kadonaga, N. Yasuoka, and N. Kasai, Chem. Commun., 1597 (1971).
24. R. Mason, and A. U. M. Rae, J. Chem. Soc. (A), 1767 (1970).
25. J. M. Baraban and J. A. McGinnety, Inorg. Chem., 13, 2864 (1974).
26. S. C. Nyburg, and P. T. Cheng, Can. J. Chem., 50, 912 (1972).
27. P. T. Cheng, C. D. Cook, C. H. Koo, S. C. Nyburg, and M. T. Shiomi, Acta. Crystallogr., B27, 1904 (1971).
28. K. Okamoto, Y. Kai, N. Yasuoka, and N. Kasai, J. Organometal. Chem., 65, 427 (1974).
29. T. Kashiwagi, N. Yasuoka, T. Ueki, N. Kasai, S. Takahashi, and N. Hagihara, Bull. Chem. Soc. Jpn., 41, 296 (1968).
30. D. L. Thorn, private communication.
31. M. Elian and R. Hoffmann, Inorg. Chem.,14, 1958 (1975).
32. D. M. P. Mingo, Advan. Organometal. Chem., 15, 1 (1977).
33. S. Inagaki, H. Fujimoto, and K. Fukui, J. Am. Chem. Soc., 98, 4054 (1976).
34. L. J. Guggenberger, Inorg. Chem., 12, 499 (1973).
35. C. A. Tolman, Chem. Rev., 77, 313 (1977).
36. T. Yoshida, T. Yamagata, T. H. Tulip, J. A. Ibers, and S. Otsuka, J. Am. Chem. Soc., 100, 2063 (1978).
37. For example, J. C. Poulin, T. P. Dang, and H. B. Kagan, J. Organometal. Chem., 84, 87 (1975).